Inorganic Chemistry

Article

pubs.acs.org/IC

Molybdenum Trihydride Complexes: Computational Determinations of Hydrogen Positions and Rearrangement Mechanisms

Lukasz Szatkowski and Michael B. Hall*

Department of Chemistry, Texas A&M University, College Station, Texas 77843, United States

Supporting Information

ABSTRACT: In crystal structures of the molybdenum complexes $[(1,2,4\text{-}C_5H_2{}^tBu_3)Mo(PMe_3)_2H_3]$ (Cp^tBu_3) and $[(C_5H^iPr_4)Mo(PMe_3)_2H_3]$ (Cp^iPr_4), the Mo-bound hydrogen positions were resolved for Cp^tBu_3, but not for Cp^iPr_4. NMR experiments revealed the existence of an unknown mechanism for hydrogen atom exchange in these molecules, which can be "frozen out" for Cp^tBu_3 but not for Cp^iPr_4. Density functional theory calculations of the most stable conformations for both complexes in the gas phase and in a continuum solvent model indicate that the H's of the Cp^iPr_4 complex are unresloved because of their disorder, which does not occur for Cp^tBu_3. A corresponding examination of alternative rearrangement pathways shows that the rearrangements of the H's could occur by two mechanisms: parallel to the cyclopentadienyl (Cp) ring in a single step and perpendicular to the Cp ring in two steps. The parallel pathway is preferred for both molecules, but it has a lower energy barrier for Cp^iPr_4 than for Cp^tBu_3.

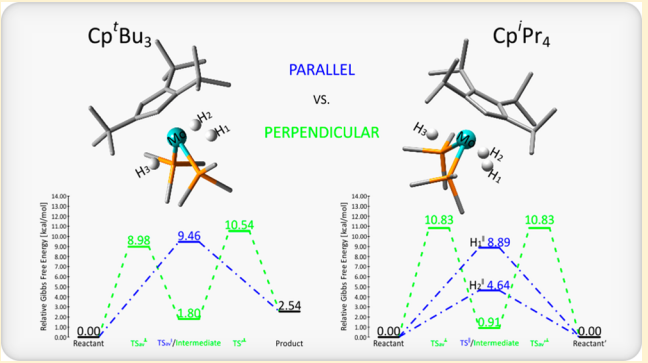

INTRODUCTION

Experimental[1] and theoretical[2,3] investigations have played a key role in explaining the differences in reactivity and stability of transition-metal dihydrogen (nonclassical) and dihydride (classical) complexes. However, aspects of their rearrangement mechanisms and the nature of the so-called stretched dihydrogen bond,[4] which shows intermediate bond lengths between classical and nonclassical cases, have yet to be thoroughly explained. Two new sterically protected molybdenum trihydride complexes, $[(1,2,4\text{-}C_5H_2{}^tBu_3)Mo(PMe_3)_2H_3]$ (Cp^tBu_3) and $[(C_5H^iPr_4)Mo(PMe_3)_2H_3]$ (Cp^iPr_4), were synthesized and crystallized by Baya et al. in 2007 (see Figure 1).[5,6] Unfortunately, crystallography was unable to define positions for the three crucial hydrogens in the Cp^iPr_4 complex. However, the NMR spectra[6] appear to show high similarity between the Cp^tBu_3 and Cp^iPr_4 complexes.

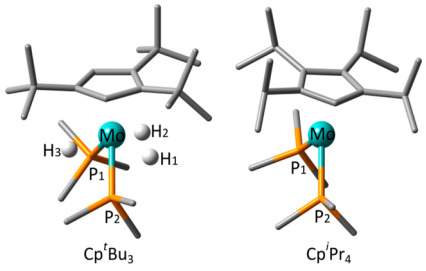

Figure 1. Crystal structures from the Cambridge Crystallographic Data Centre.

The room-temperature NMR for both compounds showed coupling of three protons with ^{31}P nuclei and, additionally, one sharp triplet signal on the ^1H NMR spectrum. At 193 K the hydrogen signal was completely resolved for Cp^tBu_3, while that for Cp^iPr_4 remained broad.[6] Moreover, the ^{31}P NMR signals from phosphine groups of Cp^tBu_3 were sharp and corresponded well with what would be expected from the crystal structure. On other hand, decoalescence of the protons was observed at low temperatures for Cp^iPr_4. Baya et al.[6] suggested that the source of this observation could be inequivalent PMe_3 groups or an equilibrium between two Cp^iPr_4 rotamers with different ^{i}Pr conformations. However, they assumed that the first case was less likely because they did not observed even a small P−P coupling at 193 K.

This paper explains of the unusual behavior of these two complexes on the basis of theoretical reaction modeling with density functional theory (DFT).

COMPUTATIONAL DETAILS

All calculations were performed using Gaussian 09 (RevD.01) software[7] with very tight convergence criteria in the gas phase (GP) and with the SMD continuum solvent models for tetrahydrofuran (THF) and acetonitrile (MeCN).[8] Restricted DFT electronic structure calculations, geometry optimization, and frequency calculation were performed for closed-shell diamagnetic complexes with the hybrid B3LYP functional[9−11] and the range-separated hybrid ωB97X-D functional[12] with several basis sets: BS1 is SDD basis set with effective core potentials (ECP);[13−15] BS2 is the Pople 6-31+G(d,p) basis

Received: March 27, 2015
Published: June 23, 2015

DOI: 10.1021/acs.inorgchem.5b00693
Inorg. Chem. 2015, 54, 6380−6385

set[16−20] on carbon, hydrogen, and phosphorus and SDD basis set with effective core potentials (ECP)[13−15] for the molybdenum; and BS3 is the 6-311+G(d,p) basis set[21−23] on all atoms except Mo. B3LYP was chosen because it is so common and because it is a reasonable compromise between computing cost and accuracy for transition metals,[24] while ωB97X-D, which contains Grimme's empirical corrections to dispersion, was chosen because it has recently been shown to be much more accurate for organometallic complexes with transition metals.[25]

RESULTS AND DISCUSSION

Cp^tBu_3 and Cp^iPr_4 Minima. A series of initial scans (rotations of Cp groups, PMe_3 groups, and H atom exchanges) for both species, Cp^tBu_3 and Cp^iPr_4, were performed with the B3LYP functional and BS1 in the gas phase. From those results, five of the lowest electronic energy structures were chosen for each compound for further reoptimization with the B3LYP and ωB97X-D functional in BS2 and BS3. On the basis of Gibbs free energy of these reoptimized structures with both B3LYP and ωB97X-D functionals in both gas phase and SMD continuum solvent models with tetrahydrofuran (THF) and acetonitrile (MeCN), two minima were found for Cp^tBu_3, which are referred to as "reactant" (lower energy structure) and as "product", while only one ("reactant") was found for Cp^iPr_4 (see Supporting Information (SI), section S.I).

The reactant structures are shown in Figure 2, and their geometries are compared to the experimental ones in Table 1.

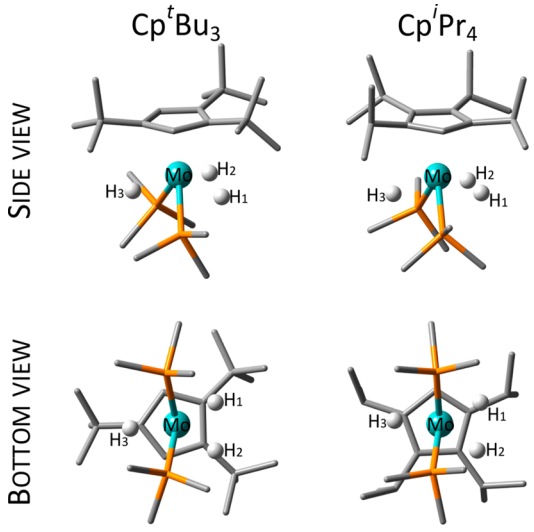

Figure 2. Positions of hydrogens atoms in Cp^tBu_3 and Cp^iPr_4 in GP B3LYP/6-31+G(d,p)/SDD for the most stable reactant structures. For clarity, no hydrogens atoms, except those connected with the Mo atom, are shown.

It can be concluded that both functionals produced bond distances and angles that compared favorably with those from the crystal structures. Generally, the Mo−X distances from the ωB97X-D calculations are slightly shorter that those from the B3LYP. When compared with the experimental structures (Mo−H distances can only be compared with the more accurate neutron diffraction), the ωB97X-D produces more accurate Mo−P distances while B3LYP produces more accurate Mo−H distances (see section S.II of the SI for more data). The calculations show that the H positions, relative to the phosphines, are similar for both Cp^iPr_4 and Cp^tBu_3 (Figure 2). For both calculated structures, one of the hydrogen atoms from the H1−H2 pair is closer to the central Mo atom than the other one. However, the neutron diffraction results for Cp^tBu_3 do not show this difference because its existence arises from the calculation of one of two mirror-image forms that are averaged in the neutron structure, by vibrations and/or disorder (compare structures of reactants 1 and 2 in section S.II of the SI). Also the crucial H1−H2 distance is slightly shorter in Cp^iPr_4 molecule than in Cp^tBu_3 (Table 1). Theoretical investigations of similar complexes[26,27] produced distances in agreement with our structures, and a molecular dynamic simulation study confirmed a high probability of trihydride structures for related Mo complexes.[28] Full sets of geometrical data for all compounds in GP, THF, and MeCN as well as superposition of the most stable calculated structures with the experimental ones are given in section S.II of the SI.

Because of the steric clash between the phosphines and the large ring substituents, the most stable structures (Figure 2) show the least sterically encumbered Cp carbon atom(s) eclipsing the phosphine ligands. Although the ring positions are quite different in these two complexes, in both the Hs are arranged in a plane parallel to the Cp ring with one H on one side of the P−Mo−P plane and two H's on the other side. With this relationship between the Cp and the P−Mo−P plane, it is clear that moving one H to the other side of the P−Mo−P plane will result in a different structure for Cp^tBu_3 but the mirror-image structure for Cp^iPr_4. Thus, for Cp^tBu_3 this H rearrangement produces the less stable product, which is calculated to be on average ∼2−3 kcal/mol higher in energy, but the reactant complex will have a single stable geometry (apart from the Mo−H distances mentioned above) in the crystal structure (see the SI). However, for Cp^iPr_4 such a reversal of H positions results in its optical enantiomer with the same energy (see the SI). Thus, there will be two energetically degenerate structures with different H positions in the crystal structure of Cp^iPr_4; this disorder of the H's in Cp^iPr_4 accounts for the inability to refine their positions in the crystal structure.

Hydrogen Rearrangement. The NMR results for both Cp^tBu_3 and Cp^iPr_4 show that there must exist reaction pathways leading to rapid exchange among the hydrogen atoms bound to molybdenum. Numerous alternative pathways for the exchange were examined in the GP by B3LYP/BS2. This examination discovered that the two lowest energy pathways for both complexes involve H motion parallel and perpendicular to the cyclopentadienyl ring (Figure 3). The key feature of the rearrangement to exchange the H's must be the exchange of the unique H on one side of the P−Mo−P plane (H3) with the other H's (H1 and H2). In the parallel rearrangements for Cp^tBu_3 (top of Figure 3), the H2 atom in the reactant moves in a plane parallel to the Cp ring over a transition state ($TS^{\parallel}$), where H2 is in the P−Mo−P plane between one of the P atoms and the Cp ring, to the product, which is not equivalent to the reactant but is the other low-energy isomer mentioned above. Finally, H3 moves back over the same $TS^{\parallel}$ (like the reverse reaction for H1) to return to the most stable isomer; continued motion along this path results in complete exchange of the H's. Note that the phosphine ligand rotates and the Mo−P bond elongates as the H passes over it in $TS^{\parallel}$. In the product, the P−Mo−P plane has tilted away from the newly formed hydrogen atom pair H2−H3. In the perpendicular rearrangements (next set down in Figure 3), the H2 atom moves away from the Cp ring over $TS^{\perp}$, where H2 approaches the P−Mo−P plane and the P−Mo−P angle opens up by 16.9° relative to the reactant. Here, $TS^{\perp}$ leads to an

DOI: 10.1021/acs.inorgchem.5b00693
Inorg. Chem. 2015, 54, 6380−6385

Table 1. Comparison of X-ray and Neutron Diffraction Structures of Cp^tBu_3 and Cp^iPr_4 and Theoretical Ones in GP with 6-31+G(d,p) and 6-311+G(d,p) Basis Sets for H, C, and P

	B3LYP		ωB97X-D			
bond lengths (Å) or angles (deg)	6-31	6-311	6-31	6-311	X-ray[a]	neut. diff.[a]
			Cp^tBu_3			
Mo−H1	1.714	1.714	1.705	1.705	1.580(30)	1.719(09)
Mo−H2	1.690	1.691	1.686	1.686	1.576(30)	1.719(10)
Mo−H3	1.715	1.715	1.710	1.709	1.578(30)	1.712(08)
H1−H2	1.737	1.732	1.700	1.700	1.632(40)	1.692(10)
P1−Mo	2.429	2.431	2.389	2.390	2.380(01)	2.377(05)
P2−Mo	2.440	2.441	2.395	2.394	2.383(01)	2.385(06)
H1−Mo−H2	61.4	61.2	60.2	60.2	62.3(2.0)	59.0(0.4)
P1−Mo−P2	93.8	93.7	94.3	94.1	93.7(0.0)	93.6(0.2)
			Cp^iPr_4			
Mo−H1	1.695	1.695	1.690	1.689		
Mo−H2	1.701	1.702	1.694	1.694		
Mo−H3	1.721	1.721	1.719	1.719		
H1−H2	1.713	1.708	1.692	1.690		
P1−Mo	2.435	2.437	2.392	2.392	2.376(04)	
P2−Mo	2.437	2.439	2.397	2.397	2.374(04)	
H1−Mo−H2	60.6	60.4	60.0	59.9		
P1−Mo−P2	94.4	94.2	94.0	93.8	94.0(0.1)	

[a]Data read in Mercury 3.3 from crystal structures from the Cambridge Crystallographic Data Centre via www.ccdc.cam.ac.uk/data_request/cif; digits measuring uncertainty are given in parentheses.

"intermediate", where the H2 lies between the phosphines nearly in the P−Mo−P plane. Note that here, in the Cp^tBu_3 molecule, the H2 atom has not yet crossed the P−Mo−P plane. There is then another transition state ($TS'^{\perp}$) that transfers the H through the P−Mo−P plane and connects the intermediate to the product, identical to the one from the parallel rearrangement. The $TS'^{\perp}$ for perpendicular rearrangement looks very similar to the earlier $TS^{\perp}$; the only difference is the location of the "transferring" H atom on the opposite side of the P−Mo−P plane. Therefore, $TS'^{\perp}$ is connected to a higher reaction barrier than $TS^{\perp}$ due to fact that the H atom must cross the P−Mo−P plane.

The reaction pathways for the Cp^iPr_4 molecule are similar (lower two sections of Figure 3). Here, the motion of hydrogen H2 results in two symmetric (C_s) TSs for the parallel motion and a symmetric (C_s) intermediate for the perpendicular pathway. Thus, both pathways will exchange the H's and produce the other enantiomer of the reactant. In the parallel pathway, there are two alternative TSs, where the transferring H is trans (shown in Figure 3) or cis (not shown in Figure 3) to the unique C in the Cp ring. In the perpendicular pathway, the high symmetry of the intermediate species results in two mirror-image $TS^{\perp}$s on both sides of the intermediate. Note that in both of these pathways one of the phosphine ligands undergoes a rotation as H2 moves.

With the Mo atom at the center of the polyhedron, the geometry of each reactant/product structure can be described as a trigonal prism with the Cp ring taking one vertex, while the transition-state structures (of both parallel and perpendicular pathways) and intermediate structures can be assigned to two different octahedron; for more discussion and illustrations, see section S.III in the SI.

Energy diagrams for these rearrangements are shown in Figure 4; additional energy data are available in the SI. For the Cp^tBu_3 molecule, the lowest transition-state barrier is for the perpendicular transfer ($TS^{\perp}$) of H1 or H2 to the intermediate; however, the next transition state on this path ($TS'^{\perp}$) is higher in energy than the transition state for the parallel rearrangement ($TS^{\parallel}$). Thus, the complete exchange of the H's for the Cp^tBu_3 molecule occurs via the parallel pathway. However, the reverse reaction in the perpendicular rearrangement from the intermediate to the reactant could lead to a structure identical with reactant, but with H1 and H2 exchanged. This part of the path could participate in the overall exchange process. It should be noted that there are often several very similar structures but with slightly different energies because of the various methyl group rotamers that are possible (see the SI). The relative activation energy between these nearly identical structures should be small enough to ensure fast dynamic exchange between them.

The situation for Cp^iPr_4 is somewhat different. Although the barriers for the two alternative parallel pathways for exchange of H3 with H1 and H2 lead to identical products, there is a significant difference between the barriers for these two pathways (see Figure 4). We believed that the higher energy transition state ($TS^{\parallel}$) for H1 moving under the C−H bond of the Cp ring is caused by steric hindrance in the transition-state structure connected with larger changes of P−Mo−P angle and Mo−P distances. In both $TS^{\parallel}$s, the hydrogen atom passing above the phosphine group forces it to rotate and to tilt away from the Cp ring (see Figure 5). A similar issue does not exist for the perpendicular rearrangement, where H1 or H2 moves down between the phosphine groups through identical transition states ($TS^{\perp}$) for either H1 or H2 to an intermediate with one of the H's exactly in the P−Mo−P plane. Further transfer of H1 or H2 atom from the intermediate proceeds through the same activation barrier ($TS^{\perp}$) (see Figure 4). Therefore, for Cp^iPr_4, there are three possible pathways that can lead to exchange of molybdenum's hydrogen positions, but one of the two parallel pathways is approximately 2.7 kcal/mol lower than any of the others. A full energy diagram can be found in Figure S10 of the SI. Moreover, changing the Mo basis set from SDD to LANL2TZ(f)[29−33] did not lead to any further improvements of the energy diagrams; see Table S13 of the SI.

DOI: 10.1021/acs.inorgchem.5b00693
Inorg. Chem. 2015, 54, 6380−6385

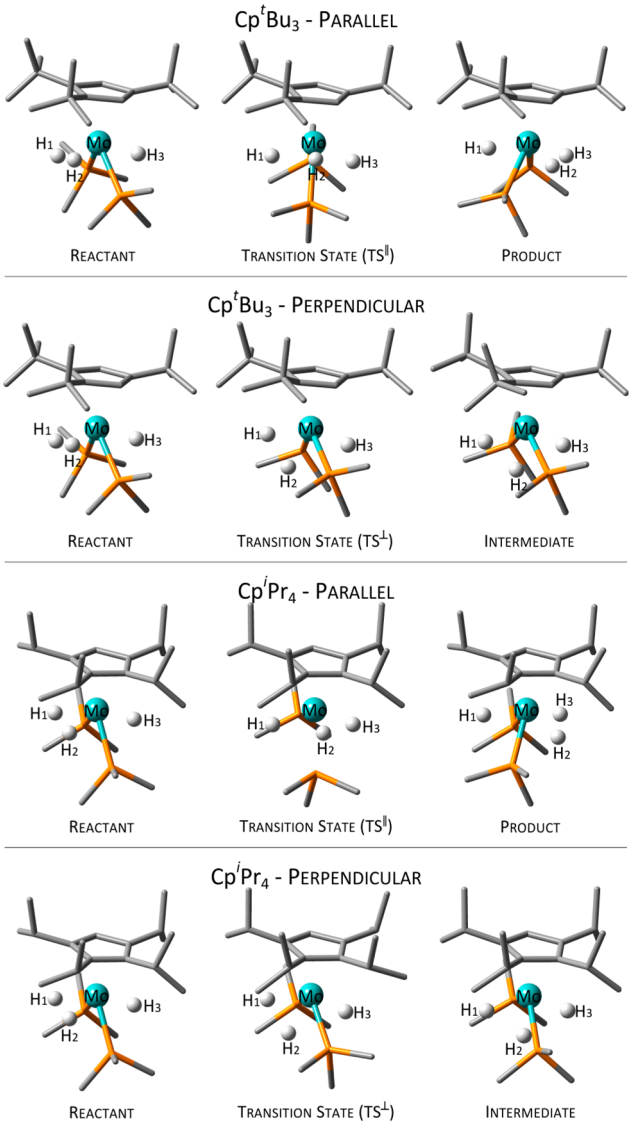

Figure 3. Reactants, transition states, products, and intermediates for the parallel rearrangement and the first stage of the perpendicular rearrangement for H2 in Cp^{t}Bu$_3$ and Cp^{i}Pr$_4$ in GP B3LYP/6-31+G(d,p)/SDD. For clarity, no hydrogen atoms, except those connected with Mo atom, are shown.

One also might expect to find a low-energy pathway for the exchange of the two hydrogen atoms on the same side of the P−Mo−P plane, namely, H1 and H2. Exchanges like this typically occur through reductive elimination to the form a dihydrogen complex, rotation of the H_2, and oxidative addition back to the reactant complex. In this process there would be a transition state (TS^{R1}) to form the dihydrogen intermediate, then another transition state (TS^{R2}) for H_2 rotation, and, finally, back through TS^{R1} to re-form the dihydride (Figure 6). Although this sequence of steps was found for the Cp^{t}Bu$_3$ molecule (Figure 7), for the Cp^{i}Pr$_4$ molecule, the H1−H2 exchange occurs without formation of the metastable dihydrogen complex. In this case, only TS^{R2} was found, but the H−H distance in this transition state was also short, as if the H_2 complex was a precursor (0.899 and 0.912 Å, respectively, for Cp^{t}Bu$_3$ and Cp^{i}Pr$_4$ in TS^{R2}). These values correspond well with a recent theoretical report for a similar reaction in Ru tryhidride complexes.[34] Even for the Cp^{t}Bu$_3$

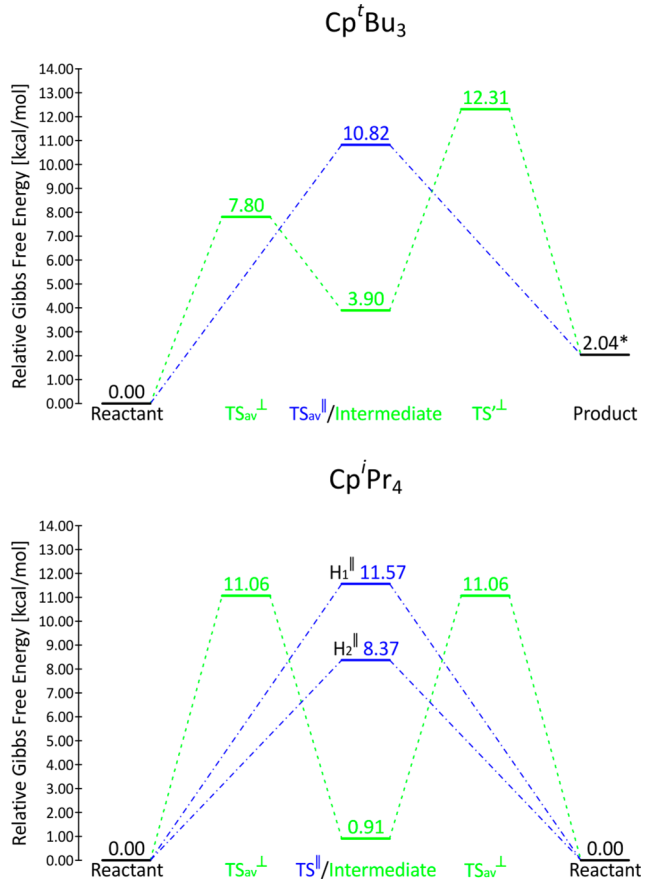

Figure 4. Gas-phase free energy diagram for reactants, transition states, intermediates and products/reactants' structures for parallel (blue) and perpendicular (green) rearrangement of H1 and H2 atom in Cp^{t}Bu$_3$ and Cp^{i}Pr$_4$ in B3LYP/6-31+G(d,p)/SDD. TS_{av} is an average value from two energetically similar TS structures (for H1 and H2), while * denotes the product with the lowest energy from all found for Cp^{t}Bu$_3$ molecule.

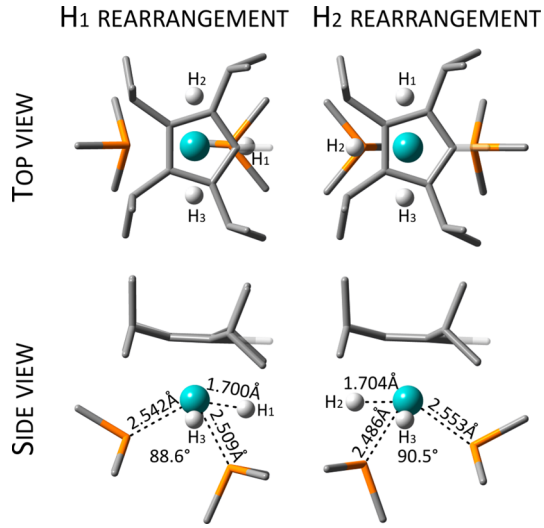

Figure 5. Top and side view for transition states of parallel rearrangement ($TS^{\perp}$) of H1 and H2 atom in Cp^{i}Pr$_4$ in GP B3LYP/6-31+G(d,p)/SDD with key distances and angles. For clarity hydrogen atoms are not shown, except those connected to the Mo atom and directly to the Cp ring.

DOI: 10.1021/acs.inorgchem.5b00693
Inorg. Chem. 2015, 54, 6380−6385

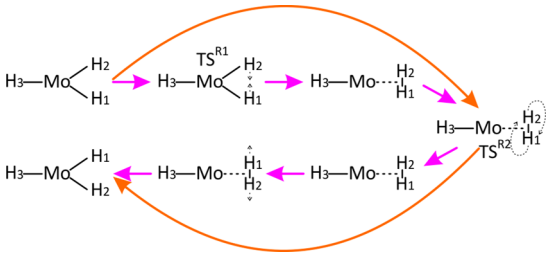

Figure 6. Scheme for exchange between the two hydrogen atoms on the same side of the P−Mo−P plane through a dihydrogen-like structure for Cp^tBu_3 (pink arrows) and Cp^iPr_4 (orange arrows).

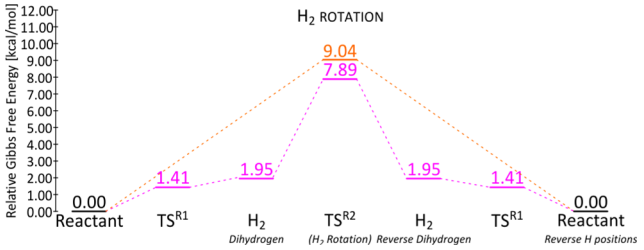

Figure 7. Free energy diagram of exchange positions between two hydrogen atoms in GP B3LYP/6-31+G(d,p)/SDD for Cp^tBu_3 (pink) and Cp^iPr_4 (orange).

molecule, the Gibbs free energy diagram (Figure 7) shows that TS^{R1} has a lower energy than the H_2 complex. The energy of TS^{R1} is only above that of the H_2 complex (TS^{R1} = 2.65 kcal/mol, H_2 complex = 2.64 kcal/mol) for the electronic energy. A TS^{R1}-like structure may also exist for Cp^iPr_4, but because of its different steric and electronic properties, a stable dihydrogen complex does not exist.

Influence of Solvent. The influence of solvent was investigated by reoptimizing the structures for the hydrogen rearrangements with the SMD continuum solvation model, with both B3LYP and ωB97X-D functionals and with BS2. In the reactant structure, the H1−H2, Mo−P1, and Mo−P2 distances are the most sensitive to changes in the environment, and they all become longer when the environment becomes more polar (from GP through THF to MeCN). The increase of the H1−H2 distances is connected with dilation of the H1−Mo−H2 angle, while the elongation of Mo−P bonds is usually accompanied by reduction of the P1−Mo−P2 angle (see Tables S1−S12 and Figure S8 of the SI). As shown in Table 2, the largest free energy stabilizations are observed for all transition-state structures in the parallel rearrangement ($TS^{\parallel}$) for both molecules (see Tables S15 and S16 of the SI for the solvation energies themselves).

The free energy change with solvation corrections did not changed our earlier conclusion about the preferred reaction path for Cp^tBu_3 molecule (Table 2). While the first energy barrier $\Delta G(\perp)^{\ddagger}$ may suggest that perpendicular rearrangement is preferred, the higher energy of the second one, $\Delta G(\perp')^{\ddagger}$, leads us to the same conclusion as discussed earlier for the gas phase, namely, that the one-step parallel exchange mechanism is preferred. Generally, the TS for the parallel pathway is stabilized most by solvation, while the second most strongly stabilized species is the intermediate in the perpendicular pathway. Thus, the solvation corrections lower the barrier for the parallel pathway and increase the barrier for the perpendicular pathway. Similar stabilizations are observed for the Cp^iPr_4 molecule, where solvation corrections bring down the barriers for both parallel pathways (H1 and H2) such that they are both below that for the perpendicular pathway. Thus, the parallel rearrangement is clearly preferred, and the difference between activation energies of the parallel [$\Delta G(\parallel)^{\ddagger}$] and perpendicular rearrangement [$\Delta G(\perp)^{\ddagger}$] are larger for Cp^iPr_4 than for Cp^tBu_3. Moreover, theoretical enthalpy values in THF solvent for parallel pathways for both compounds [Cp^tBu_3, 7.83 kcal/mol for B3LYP/BS2 and 9.49 kcal/mol for ωB97X-D/BS2; Cp^iPr_4 (rate-determining step for H1 atom), 5.53 kcal/mol for B3LYP/BS2 and 6.71 kcal/mol for ωB97X-D/BS2; also see Table S17] are in good agreement with the experimental enthalpy values for the hydride-scrambling process (9.0 ± 0.7 and 8.5 ± 0.3 kcal/mol, respectively, for Cp^tBu_3 and Cp^iPr_4).[6]

The free-energy calculations (Table 2) predict a more rapid H exchange for Cp^iPr_4 over that for Cp^tBu_3 in acetonitrile by nearly 2 orders of magnitude. Thus, our modeling explains the NMR results of Baya et al.[6] that even at low temperatures (193 K) the fast hydrogen exchange in the parallel mechanism of Cp^iPr_4 prevents the final resolution of the NMR signal. Moreover, because of the rapid parallel exchange in Cp^iPr_4, its

Table 2. Gibbs Free Energies for Activations ($\Delta G^{\ddagger}$) and Reactions to Products (ΔG^{P}), Reactants (ΔG^{R}), and Intermediates (ΔG^{I}) for Parallel (∥) and Perpendicular (⊥) Reactions[a]

	Cp^tBu_3 (kcal/mol)									
	B3LYP/6-31+G(d,p)/SDD					ωB97X-D/6-31+G(d,p)/SDD				
	$\Delta G(\parallel)^{\ddagger}$	$\Delta G(\perp)^{\ddagger}$	$\Delta G(\perp)^{I}$	$\Delta G(\perp')^{\ddagger}$	ΔG^{P}	$\Delta G(\parallel)^{\ddagger}$	$\Delta G(\perp)^{\ddagger}$	$\Delta G(\perp)^{I}$	$\Delta G(\perp')^{\ddagger}$	ΔG^{P}
GP	10.74	8.25	3.90	12.31	2.04	12.31	8.95	3.81	13.32	2.74
THF	9.20	8.29	3.70	12.44	1.63	10.94	9.06	2.98	11.37	2.76
MeCN	7.87	6.80	1.32	11.35	1.48	9.46	8.98	1.80	10.54	2.54
	Cp^iPr_4 (kcal/mol)									
	B3LYP/6-31+G(d,p)/SDD					ωB97X-D/6-31+G(d,p)/SDD				
	$\Delta G^{H1}(\parallel)^{\ddagger}$	$\Delta G^{H2}(\parallel)^{\ddagger}$	$\Delta G(\perp)^{\ddagger}$	$\Delta G(\perp)^{I}$	ΔG^{R}	$\Delta G^{H1}(\parallel)^{\ddagger}$	$\Delta G^{H2}(\parallel)^{\ddagger}$	$\Delta G(\perp)^{\ddagger}$	$\Delta G(\perp)^{I}$	ΔG^{R}
GP	11.57	8.37	11.47	0.91	0.10	11.40	9.08	11.29	−0.89	−0.55
THF	10.81	5.71	11.98	−0.51	0.08	9.67	6.93	11.07	−1.63	−0.66
MeCN	8.89	4.64	10.83	−2.08	0.06	7.79	5.36	11.03	−3.31	−0.88

[a]Due to the high degree of similarity between the hydrogen atoms H1 and H2, the table only provides the Gibbs free energy for the H2 hydrogen atom, except in the case of parallel pathways for Cp^iPr_4 molecule, where we show separate energy barriers for H1 and H2, because these transition states have totally different geometries; see Figure 5.

DOI: 10.1021/acs.inorgchem.5b00693
Inorg. Chem. 2015, 54, 6380−6385

crystal structures is a racemate, which prevented the resolution of the H atom positions. Interestingly, the symmetric intermediate in the perpendicular pathway for $Cp^{i}Pr_4$ is stabilized below the energy of the reactant structure, which is observed in the crystal. Because of the large difference in the P−Mo−P angle for these two species, we know that the intermediate cannot be playing a role in the solid state but speculate that it might have some role in a high polarity solvent. It is possible that the same intermediate, in which the H atom is between two PMe_3 groups, blocking their interactions, may be also responsible for a decoalescence of ^{31}P NMR signals. Alternatively, this decoalescence might be due to the slowing of the Cp ring rotation, which has a relatively low barrier (approximately 10.13 kcal/mol in GP/B3LYP/BS2), in the $Cp^{i}Pr_4$ molecule (for more details see section S.VI of the SI). Of course, such ring rotations cannot exchange the H's.

SUMMARY AND CONCLUSIONS

In summary, DFT calculations successfully predicted and explained the missing hydrogen positions in the crystal structure of $Cp^{i}Pr_4$. Further, these calculations identified two possible hydrogen exchange mechanisms for both $Cp^{t}Bu_3$ and $Cp^{i}Pr_4$ complexes and predicted that the pathway in which the hydrogens exchange by moving parallel to the Cp ring has the lowest energy. The lower barriers for this process in the case of $Cp^{i}Pr_4$ explain why, even at low temperature, the NMR signals are still unresolved.

ASSOCIATED CONTENT

Supporting Information

Geometrical and energetic data and Cartesian coordinates of structures from the gas phase. The Supporting Information is available free of charge on the ACS Publications website at DOI: 10.1021/acs.inorgchem.5b00693.

AUTHOR INFORMATION

Corresponding Author

*E-mail: hall@science.tamu.edu.

Author Contributions

The manuscript was written through contributions of all authors. All authors have given approval to the final version of the manuscript. Authors contributed equally.

Notes

The authors declare no competing financial interest.

ACKNOWLEDGMENTS

The authors acknowledge the support of this work by The Welch Foundation (Grant A-0648) and Texas A&M University's Supercomputer Facility. They also thank Ivica Milovanovic for preliminary calculations on these molecules while a Visiting Scholar at Texas A&M University.

REFERENCES

(1) Kubas, G. *Chem. Rev.* **2007**, *107*, 4152−4205.
(2) Zhenyang, L.; Hall, M. *Coord. Chem. Rev.* **1994**, *135/136*, 845−879.
(3) Besora, M.; Lledós, A.; Maseras, F. *Chem. Soc. Rev.* **2009**, *38*, 957−966.
(4) Heinekey, D.; Lledós, A.; Lluch, J. *Chem. Soc. Rev.* **2004**, *33*, 175−182.
(5) Baya, M.; Houghton, J.; Daran, J.; Poli, R. *Angew. Chem., Int. Ed.* **2007**, *46*, 429−432.
(6) Baya, M.; Houghton, J.; Daran, J.; Poli, R.; Male, L.; Albinati, A.; Gutman, M. *Chem.—Eur. J.* **2007**, *13*, 5347−5359.
(7) Frisch, M. J.; Trucks, G. W.; Schlegel, H. B.; Scuseria, G. E.; Robb, M. A.; Cheeseman, J. R.; Scalmani, G.; Barone, V.; Mennucci, B.; Petersson, G. A.; Nakatsuji, H.; Caricato, M.; Li, X.; Hratchian, H. P.; Izmaylov, A. F.; Bloino, J.; Zheng, G.; Sonnenberg, J. L.; Hada, M.; Ehara, M.; Toyota, K.; Fukuda, R.; Hasegawa, J.; Ishida, M.; Nakajima, T.; Honda, Y.; Kitao, O.; Nakai, H.; Vreven, T.; Montgomery, J. A., Jr.; Peralta, J. E.; Ogliaro, F.; Bearpark, M.; Heyd, J. J.; Brothers, E.; Kudin, K. N.; Staroverov, V. N.; Kobayashi, R.; Normand, J.; Raghavachari, K.; Rendell, A.; Burant, J. C.; Iyengar, S. S.; Tomasi, J.; Cossi, M.; Rega, N.; Millam, J. M.; Klene, M.; Knox, J. E.; Cross, J. B.; Bakken, V.; Adamo, C.; Jaramillo, J.; Gomperts, R.; Stratmann, R. E.; Yazyev, O.; Austin, A. J.; Cammi, R.; Pomelli, C.; Ochterski, J. W.; Martin, R. L.; Morokuma, K.; Zakrzewski, V. G.; Voth, G. A.; Salvador, P.; Dannenberg, J. J.; Dapprich, S.; Daniels, A. D.; Farkas, Ö.; Foresman, J. B.; Ortiz, J. V.; Cioslowski, J.; Fox, D. J. *Gaussian 09, Revision D.01*; Gaussian, Inc., Wallingford, CT, 2009.
(8) Marenich, A.; Cramer, C.; Truhlar, D. *J. Phys. Chem. B* **2009**, *113*, 6378−6396.
(9) Becke, A. *J. Chem. Phys.* **1993**, *98*, 5648−5652.
(10) Lee, C.; Yang, W.; Parr, R. *Phys. Rev. B* **1988**, *37*, 785−789.
(11) Stephens, P.; Devlin, F.; Chabalowski, C.; Frisch, M. *J. Phys. Chem.* **1994**, *98*, 11623−11627.
(12) Chai, J.; Head-Gordon, M. *Phys. Chem. Chem. Phys.* **2008**, *10*, 6615−6620.
(13) Dunning, T. H., Jr.; Hay, P. J. In *Modern Theoretical Chemistry*, Schaefer, H. F., III, Ed.; Plenum: New York, 1977; Vol. 3, pp 1−28.
(14) Fuentealba, P.; Preuss, H.; Stoll, H.; Von Szentpály, L. *Chem. Phys. Lett.* **1982**, *89*, 418−422.
(15) Andrae, D.; Haeussermann, U.; Dolg, M.; Stoll, H.; Preuss, H. *Theor. Chem. Acc.* **1990**, *77*, 123−141.
(16) Hariharan, P.; Pople, J. *Theor. Chem. Acc.* **1973**, *28*, 213−222.
(17) Ditchfield, R.; Hehre, W.; Pople, J. *J. Chem. Phys.* **1971**, *54*, 724−728.
(18) Francl, M.; Pietro, W.; Hehre, W.; Binkley, J.; Gordon, M.; DeFrees, D.; Pople, J. *J. Chem. Phys.* **1982**, *77*, 3654−3665.
(19) Clark, T.; Chandrasekhar, J.; Spitznagel, G.; Schleyer, P. *J. Comput. Chem.* **1983**, *4*, 294−301.
(20) Frisch, M.; Pople, J.; Binkley, J. *J. Chem. Phys.* **1984**, *80*, 3265−3269.
(21) McLean, A.; Chandler, G. *J. Chem. Phys.* **1980**, *72*, 5639−5648.
(22) Raghavachari, K.; Binkley, J.; Seeger, R.; Pople, J. *J. Chem. Phys.* **1980**, *72*, 650−654.
(23) McLean, A. D.; Chandler, G. S. *J. Chem. Phys.* **1980**, *72*, 5639−5648.
(24) Cramer, C. J.; Truhlar, D. G. *Phys. Chem. Chem. Phys.* **2009**, *11*, 10757−10816.
(25) Minenkov, Y.; Singstad, Å.; Occhipintia, G.; Jensen, V. R. *Dalton Trans.* **2012**, *41*, 5526−5541.
(26) Abugideiri, F.; Fettinger, J. C.; Pleune, B.; Poli, R.; Bayse, C. A.; Hall, M. B. *Organometallics* **1997**, *16*, 1179−1185.
(27) Belkova, N. V.; Revin, P. O.; Besora, M.; Baya, M.; Epstein, L. M.; Lledós, A.; Poli, R.; Shubina, E. S.; Vorontsov, E. V. *Eur. J. Inorg. Chem.* **2006**, *11*, 2192−2209.
(28) Piękoś, Ł.; Mitoraj, M. P. *J. Comput. Chem.* **2013**, *34*, 294−304.
(29) Hay, P. J.; Wadt, W. R. *J. Chem. Phys.* **1985**, *82*, 299−310.
(30) Roy, L. E.; Hay, P. J.; Martin, R. L. *J. Chem. Theory Comput.* **2008**, *4*, 1029−1031.
(31) Ehlers, A. W.; Bohme, M.; Dapprich, S.; Gobbi, A.; Hollwarth, A.; Jonas, V.; Kohler, K. F.; Stegmann, R.; Veldkamp, A.; Frenking, G. *Chem. Phys. Lett.* **1993**, *208*, 111−114.
(32) Hay, P. J.; Wadt, W. R. *J. Chem. Phys.* **1985**, *82*, 270−283.
(33) Hay, P. J.; Wadt, W. R. *J. Chem. Phys.* **1985**, *82*, 284−298.
(34) Jiménez-Tenorio, M.; Puerta, M. C.; Valerga, P.; Moncho, S.; Ujaque, G.; Lledós, A. *Inorg. Chem.* **2010**, *49*, 6035−6057.

DOI: 10.1021/acs.inorgchem.5b00693
Inorg. Chem. 2015, 54, 6380−6385